46th Annual Review of Progress in Quantitative Nondestructive Evaluation
QNDE2019
July 14-19, 2019, Portland, OR, USA

QNDE2019-1234

SIMULATED ANNEALING BASED POLARIZATION OPTIMIZATION FOR DUAL MACH-ZEHNDER INTERFEROMETER FIBER VIBRATION SENSOR

Jian Li
State Key Laboratory of Precision Measurement Technology and Instruments, Tianjin University
Tianjin, China

Hao Feng
State Key Laboratory of Precision Measurement Technology and Instruments, Tianjin University
Tianjin, China

Yu Zhang
State Key Laboratory of Precision Measurement Technology and Instruments, Tianjin University
Tianjin, China

Zhou Sha
State Key Laboratory of Precision Measurement Technology and Instruments, Tianjin University
Tianjin, China

ABSTRACT

The accurate positioning of intruding events remains a vital task in distributed oil and gas pipeline safety precaution system. Time delay, which is used for determining the intruding location is generally obtained through cross correlation. However, random evolution of polarization states cause optical signals uncorrelated and lead to great positioning deviation. In this paper, the model of the light path is established based on Jones matrix and the method of controlling correlation coefficient is discussed via adjusting the polarization state of the light. A control algorithm is proposed based on Simulated Annealing. The correlation coefficient is the feedback parameter as well as objective value. It is demonstrated that the algorithm can stabilize the correlation coefficient and eliminate the estimation error significantly.

Keywords: Phase polarization control, Mach-Zehnder fiber interferometer, polarization analysis, Simulated Annealing

1. INTRODUCTION

Oil and gas pipeline safety monitoring and pre-warning system has been developed based on the dual Mach-Zehnder fiber interferometer as demonstrated in [1]. It manages to combine the interferometer's high sensitivity with distributed sensing ability. The system utilizes communication optical fibers laid parallel with the pipe as the senor to detect and locate exterior damages, e.g. illegal construction and gasoline theft along pipelines. As cross-correlation function is used to estimate time delay in positioning process, there is a strict requirement on the correlation between the two channels of the signal. However, due to the polarization induced fading and phase distortion phenomenon, whose production mechanism is illustrated in [2,3], detected signals' correlation deteriorates and locating errors occur constantly. This paper illustrates the theory of polarization-induced fading in the system by establishing an optical polarization model. It's shown that the correlation degeneracy owes to the inconsistency between two sensing fibers' polarization characteristics, which leads to the detected signals' susceptibility to polarization states of the incident light. In particular, the process describing how the azimuth and the ellipticity angle affect signals‟ correlation coefficient is deduced. It is proved feasible to enhance the correlation coefficient by carrying out polarization control. Up till now, existing polarization control algorithms are mainly aimed to eliminate the polarization mode dispersion (PMD) [4,6] in fiber optical communication system, or to control a dynamic parameter in fiber sensor system [7].

Whereas, common parallel algorithms such as genetic algorithm or particle swarm optimization is not satisfactorily efficient, since the system aims to manipulate a correlation coefficient calling for some time to calculate. So the kernel of the system's polarization control is to attain the operating point within least skips. Meanwhile, the algorithm should be capable of global research and not bound to local optimum in order to obtain the global optimal solution. Based on the above, Simulated Annealing is applied as the polarization control algorithm to search for the input polarization operating point. The algorithm causes little degeneration of detected signal's correlation in theory. Field experiments show that the operating point can be rapidly found and the correlation between the system detected signals can be continuously stabilized.

2. THEORETICAL INVESTIGATION

Fig. 1 shows the equivalent optical path of the dual Mach-Zehnder fiber interferometer sensing system. [1,3] Considering birefringence in the single-mode fiber, the two sensing arms L1, L2 can be modeled as polarization devices G1 and G2, whose Jones matrices are.

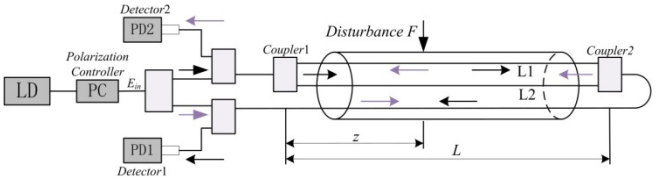

FIGURE 1: CONVENTIONAL DIAGRAM OF DUAL MACH-ZEHNDER SYSTEM STRUCTURE

$$G_1=\begin{bmatrix} e^{j\xi}\sin^2 x+\cos^2 x & \left(e^{j\xi}-1\right)\sin x\cos x \\ \left(e^{j\xi}-1\right)\sin x\cos x & e^{j\xi}\cos^2 x+\sin^2 x \end{bmatrix} \tag{1}$$

$$G_2=\begin{bmatrix} e^{j\xi'}\sin^2 x'+\cos^2 x' & \left(e^{j\xi'}-1\right)\sin x'\cos x' \\ \left(e^{j\xi'}-1\right)\sin x'\cos x' & e^{j\xi'}\cos^2 x'+\sin^2 x' \end{bmatrix} \tag{2}$$

Where x is the angle between fast axis and X axis, ξ denotes the phase retardation angle caused by fiber birefringence [3,5].Taking no account of insertion loss, when coupler's splitting ratio is 1:1, its direct coupling (ks) and cross-over coupling (ka) Jones matrices are:

$$ks=\begin{bmatrix} \frac{\sqrt{2}}{2} & 0 \\ 0 & \frac{\sqrt{2}}{2} \end{bmatrix} \quad ka=\begin{bmatrix} j\frac{\sqrt{2}}{2} & 0 \\ 0 & j\frac{\sqrt{2}}{2} \end{bmatrix} \tag{3}$$

The system's incident light can be represented by:

$$E_{in}=\begin{bmatrix} E_x \\ E_y \end{bmatrix}=E_0\begin{bmatrix} \cos\theta\cos\varepsilon-j\sin\theta\sin\varepsilon \\ \sin\theta\cos\varepsilon+j\cos\theta\sin\varepsilon \end{bmatrix} \tag{4}$$

Where E_0 denotes the light wave amplitude, θ is the azimuth, and ε is the ellipticity angle. The emergent light E_1 passing through sensing arms L_1 can be calculated by the following formula:

$$E_1=ka\times G_1\times ka\times e^{j\delta}\times E_{in} \tag{5}$$

Where δ is the phase retardation difference between two sensor fibers caused by disturbance. The orthogonal components respectively can be expanded respectively as follows:

$$\begin{aligned} E_{1x}=0.5&\left\{\begin{matrix} 0.5\sin(2x)\left[\sin(\xi)\cos(\theta)\sin(\varepsilon)+\sin(\theta)\cos(\varepsilon)-\cos(\xi)\sin(\theta)\cos(\varepsilon)\right] \\ -\sin^2(x)\left[\cos(\xi)\cos(\theta)\cos(\varepsilon)+\sin(\xi)\sin(\theta)\sin(\varepsilon)\right]-\cos^2(x)\cos(\theta)\cos(\varepsilon) \end{matrix}\right\} \\ +0.5j&\left\{\begin{matrix} 0.5\sin(2x)\left[\cos(\theta)\sin(\varepsilon)-\cos(\xi)\cos(\theta)\sin(\varepsilon)-\sin(\xi)\sin(\theta)\cos(\varepsilon)\right] \\ +\sin^2(x)\left[\cos(\xi)\sin(\theta)\sin(\varepsilon)-\sin(\xi)\cos(\theta)\cos(\varepsilon)\right]+\cos^2(x)\sin(\theta)\sin(\varepsilon) \end{matrix}\right\} \end{aligned} \tag{6}$$

$$\begin{aligned} E_{1y}=0.5&\left\{\begin{matrix} 0.5\sin(2x)\left[\cos(\theta)\cos(\varepsilon)-\cos(\xi)\cos(\theta)\cos(\varepsilon)-\sin(\xi)\sin(\theta)\sin(\varepsilon)\right] \\ +\cos^2(x)\left[\sin(\xi)\cos(\theta)\sin(\varepsilon)-\cos(\xi)\sin(\theta)\cos(\varepsilon)\right]-\sin^2(x)\sin(\theta)\cos(\varepsilon) \end{matrix}\right\} \\ +0.5j&\left\{\begin{matrix} 0.5\sin(2x)\left[\cos(\xi)\sin(\theta)\sin(\varepsilon)-\sin(\xi)\cos(\theta)\cos(\varepsilon)-\sin(\theta)\sin(\varepsilon)\right] \\ -\cos^2(x)\left[\cos(\xi)\cos(\theta)\sin(\varepsilon)+\sin(\xi)\sin(\theta)\cos(\varepsilon)\right]-\sin^2(x)\cos(\theta)\sin(\varepsilon) \end{matrix}\right\} \end{aligned} \tag{7}$$

Thus the azimuth θ_1 and the ellipticity angle ε_1 can be calculated by the follows:

$$\begin{cases} \varepsilon_1=\frac{1}{2}\arcsin\left(\frac{2\,\mathrm{Im}(X_1)}{1+|X_1|^2}\right) \\ \theta_1=\arctan\left(\frac{X_1-j\tan\varepsilon_1}{jX_1\tan\varepsilon_1+1}\right) \end{cases},\ X_1=\frac{E_{1y}}{E_{1x}} \tag{8}$$

So the E_1 can be represented as formula (9):

$$E_1=\begin{bmatrix} E_{1x} \\ E_{1y} \end{bmatrix}=E_0\exp(j\delta)\begin{bmatrix} \cos\theta_1\cos\varepsilon_1-j\sin\theta_1\sin\varepsilon_1 \\ \sin\theta_1\cos\varepsilon_1+j\cos\theta_1\sin\varepsilon_1 \end{bmatrix} \tag{9}$$

Similarly, the emergent light E_2 through the sensing arm L_2 can be represented as follows:

$$E_2=ks\times G_2\times ks\times E_{in}=E_0\begin{bmatrix} \cos\theta_2\cos\varepsilon_2-j\sin\theta_2\sin\varepsilon_2 \\ \sin\theta_2\cos\varepsilon_2+j\cos\theta_2\sin\varepsilon_2 \end{bmatrix} \tag{10}$$

where the azimuth θ_1 and the ellipticity angle ε_1 can also be calculated by formula (8). Therefore, the light E_1 out after the field superposition is:

$$E_{1out}=E_1+E_2=\begin{bmatrix} E_{1x} \\ E_{1y} \end{bmatrix}+\begin{bmatrix} E_{2x} \\ E_{2y} \end{bmatrix}=\begin{bmatrix} E_{1x}+E_{2x} \\ E_{1y}+E_{2y} \end{bmatrix} \tag{11}$$

Only considering the interference influence, the light intensity I_1 out in detector PD_1 is represented as follows:

$$\begin{aligned} I_{1out}&=|E_{out}|^2=|E_x|^2+|E_y|^2 \\ &=2E_0^2\begin{bmatrix} \cos(\delta)\cos(\theta_1-\theta_2)\cos(\varepsilon_1-\varepsilon_2) \\ +\sin(\delta)\sin(\theta_1-\theta_2)\sin(\varepsilon_1+\varepsilon_2) \end{bmatrix} \\ &=2E_0^2\cdot\sqrt{a_1^2+b_1^2}\cdot\cos(\delta-\varphi_1) \end{aligned} \tag{12}$$

Where $a_1=\cos(\theta_1-\theta_2)\cos(\varepsilon_1-\varepsilon_2)$, $b_1=\sin(\theta_1-\theta_2)\sin(\varepsilon_1+\varepsilon_2)$, $\varphi_1=\arctan(b_1/a_1)$. Similarly, the light intensity I_2 out in detector PD_2 can be represented as follows:

$$I_{2out}=2E_0^2\cdot\sqrt{a_2^2+b_2^2}\cdot\cos(\delta-\varphi_2) \tag{13}$$

Taking the length of time t of the detected signals, the correlation coefficient is calculated by the follows:

$$\rho_{xy} = \frac{\int_0^t I_{1out}(t) I_{2out}(t) dt}{\sqrt{\int_0^t I_{1out}^2(t) dt \int_0^t I_{2out}^2(t) dt}} \tag{14}$$

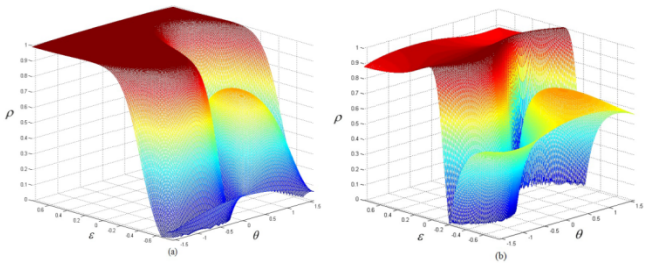

FIGURE 2: (a)RELATION BETWEEN CORRELATION COEFFICIENT AND INPUT POLARIZATION(1) (B)RELATION BETWEEN CORRELATION COEFFICIENT AND INPUT POLARIZATION(2)

Fig. 2(a) shows the relationship between the original signal's correlation coefficient ρ_{xy} and θ, ε of the input light (On the condition of ξ=1.56π, x=0.8π, ξ′=0.36π, x′=-1.14π), while fig. 2(b) shows a variation tendency along with input polarization after altering the polarization property in sensor arms L_1 and L_2 (On the condition of ξ=0.25π, x=1.25π; ξ′=π, x′=1.75π). For a monitoring and positioning system based on a dual Mach-Zehnder structure, high positioning accuracy can be guaranteed when the two detected signals' correlation coefficient $\rho_{xy} \geq 0.9$. It can be seen that coefficient ρ_{xy} varies with the azimuth angle θ and the ellipticity angle ε. By adopting appropriate polarization control algorithm in corporation with automatic polarization controller, the optimal input polarization can be found for the specific polarization state of the fiber. So it's feasible to eliminate error effects caused by polarization-induced fading and maintain a high correlation between the two signals. This input polarization state is called the polarization operating point.

2.1 Algorithm Clarification

The polarization control targets at azimuth θ and ellipticity angle ε of the incident light. Simply taking azimuth θ's effect into account, after propagating through a one-way sensor arm, the quadrature component of the emergent light at the optical coupler is depicted in formula (6)-(7). Its vertical component and horizontal component are neither even nor odd function, while arcsine and arc tangent are odd in definition domains. Consequently, the emergent light's azimuth and ellipticity angle don't have any parity properties in the domain. Further calculation infers that the interference light's intensity function received by photoelectric detectors owns no parity, either. So when azimuth θ is the sole variable, the correlation coefficient of the detected two signals in dual Mach-Zehnder fiber interferometer's two arms is not an odd or even function according to formula (10) under their given domains. The azimuth θ is defined on [-0.5π, 0.5π), during which the trigonometric function is not periodic. So after propagating through a one-way sensor arm, the incident light's vertical and horizontal component don't have any period properties in the domain, that is, the azimuth and ellipticity angle function of the emergent light are not periodic. Considering the composite function's transitivity with the period property, so is the interfered signals' intensity function. As a result, when azimuth θ is the sole variable, the correlation coefficient of the detected two signals in two arms is not periodic under given domains. Formula (15) depicts the horizontal component's derivative of the emergent light in one arm:

$$\begin{aligned} E'_{1x} = 0.5 &\left\{ \begin{array}{l} 0.5\sin(2x)\left[-\sin(\xi)\sin(\theta)\sin(\varepsilon)+\cos(\theta)\cos(\varepsilon)+\cos(\xi)\cos(\theta)\cos(\varepsilon)\right] \\ -\sin^2(x)\left[-\cos(\xi)\sin(\theta)\cos(\varepsilon)+\sin(\xi)\cos(\theta)\sin(\varepsilon)\right]+\cos^2(x)\sin(\theta)\cos(\varepsilon) \end{array} \right\} \\ +0.5j &\left\{ \begin{array}{l} 0.5\sin(2x)\left[-\sin(\theta)\sin(\varepsilon)+\cos(\xi)\sin(\theta)\sin(\varepsilon)-\sin(\xi)\cos(\theta)\cos(\varepsilon)\right] \\ +\sin^2(x)\left[\cos(\xi)\cos(\theta)\sin(\varepsilon)+\sin(\xi)\sin(\theta)\cos(\varepsilon)\right]+\cos^2(x)\cos(\theta)\sin(\varepsilon) \end{array} \right\} \end{aligned} \tag{15}$$

The relationship between the equation's real and imaginary part and zero is uncertain, so the two parts don't have any monotonicity properties in the domain. Besides, the emergent light's azimuth and ellipticity angle don't have parity or period properties, either. It can be inferred that they are not monotonous at the interval. So when azimuth θ acts as the variable, the correlation coefficient of the detected two signals in two arms is not monotonous in its domain. Similarly, when ellipticity angle ε is the sole variable, the same procedure may be easily modified to prove the correlation coefficient of the detected two signals owns no parity, period or monotonicity properties. The correlation coefficient curve of the two detected signals in two arms is shown in figure (3) when the incident light's azimuth θ or ellipticity angle ε alters as the sole variable. Curve 1 and curve 2 correspond to the settings in figure 2(a) and 2(b) respectively. When ε=0, the relationship curve between the correlation coefficient and azimuth θ is shown in figure 3(a).When θ=-1, the relationship curve between correlation coefficient and ellipticity angle ε is shown in figure 3(b).

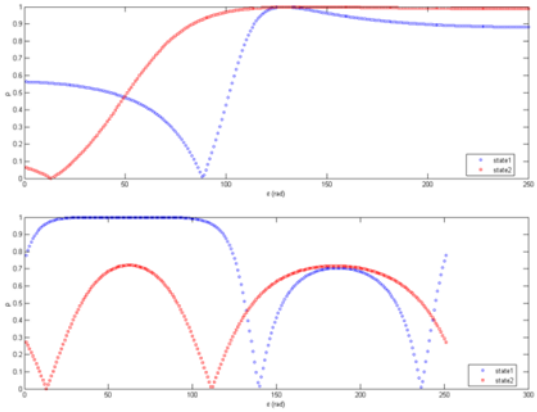

FIGURE 3: (A) E=0, RELATION BETWEEN CORRELATION COEFFICIENT AND AZIMUTH Θ (B) Θ=-1, RELATION BETWEEN CORRELATION COEFFICIENT AND ELLIPTICITY E

It's also evident that the correlation coefficient doesn't have any parity, period or monotonicity properties when azimuth θ or ellipticity angle ε varies individually in figure (3). In addition, the coefficient distribution changes with different settings. Therefore, in order to find out the operating point, a polarization control algorithm must be able to conduct global search. On the other hand, there may be more than one extreme value in the systematic objective function's multi-parameter space. Although some stationary points in figure (3) are local optima of the correlation coefficient, such as point A and B, they're not extremum over the entire domain. As a consequence, the polarization control algorithm should be able to distinguish the stationary points from extreme points to obtain the global convergence result when multiple stationary points exist simultaneously. It jumps out of saddle points and continues searching in other regions, avoiding being trapped in local optima and algorithm failure. Based on the above analysis, to achieve the desired effect, the polarization control algorithm should be capable to: 1. do global research, 2. jump out of the local optimum and get to the global optimum eventually. Any algorithm can carry out a successful research of the polarization operating point as long as it fulfills the previous requirements. Setting the differentials between correlation coefficient and desired value 1-ρxy as the objective function f(X), the polarization control model can be represented by:

$$\min(1-\rho_{xy}) = f(X) \tag{16}$$

Where X is a vector which denotes the polarization controller's four PZT channels (xi, i=1, 2, 3, 4). Thus, the problem can be considered as an optimization search process which could find the minimum f(X) within the least time in the definition domain of vector X. A polarization search and control method is proposed based on Simulated Annealing algorithm, where correlation coefficient ρ_{xy} is used as the amount of feedback control. [8, 9, 10] This method consists of two nested loops: the first loop reduces the temperature;

the second loop iterates searching the minimum f(X) for the current temperature. In addition, the method can probabilistically jump out of local optimum and achieve global optimum according to Metropolis criterion and iterate all polarization states. The steps of control algorithm are as follows:

(1) The objective function : $f(x)=1-\rho_{xy}$, sets up the initial temperature T_0 ($0<T_0\leq 1$) and the temperature update function: $F(T_k)=p_k\text{-}1 \bullet T_0$, where p is the temperature update constant; k is cycle index of the outer cycles.

(2) The polarization controller's initial control vector X_0 is initialized randomly. X_0 is the input into the polarization controller through the parallel port.

(3) The computer calculates the correlation coefficient ρ_{xy} of the two signals detected by two photoelectric detectors under the control vector X_0, and gets the target function value $f(X_0)=1-\rho_{xy}$;

(4) Set X_0, $f(X_0)$ as the algorithm's current optimization value, and set X_0, $f(X_0)$ as the global optimization value X_g and $f(X_g)$;

(5) Set the initial outer circulation counter k: k =1; set the number of outer cycles k_0, ($1<k_0\leq 10$);

(6) Set the initial inner circulation counter n: n =1; set the number of inner cycles n_0, ($1<n_0\leq 10$);

(7) The computer calculates the corresponding objective function value $f(x_n\text{-}1)$， produces a new control vector X_n according to the state producing function, and inputs X_n to the polarization controller through the parallel port, the state producing function is as follows:

$$x_n = \begin{cases} x_{n-1} - f(x_{n-1})\cdot s & x_{n-1} \geq 5\pi \\ x_{n-1} + f(x_{n-1})\cdot c\cdot s & 0 < x_{n-1} < 5\pi \\ x_{n-1} + f(x_{n-1})\cdot s & x_{n-1} \leq 0 \end{cases} \tag{17}$$

Where s in formula (17) is the maximum search step length, $0<s<2\pi$, and c is selected from -1 and 1 randomly. (8) Calculate the objective function increment $\Delta f = f(x_n) - f(x_0)$, and get the state transition probability pr according to function (18):

$$p_r(X_0 \to X_n) = \begin{cases} 1 & f(X_n) \leq f(X_0) \\ \exp(-\dfrac{\Delta f(X_n)}{T_k}) & otherwise \end{cases} \tag{18}$$

Where Tk in formula (18) is the current state temperature, and compare pr with r selected randomly from 0 to 1. If $p_r \geq r$, use Xn and $f(X_n)$ to update the current optimization value X_0 and $f(X_0)$. Otherwise, keep the current optimization value unchanged.

(9) Compare current optimization value X_0 and $f(X_0)$ with global optimization value X_g and $f(X_g)$. If $f(X_0)$ is less than $f(X_g)$, use the current optimization value X_0 and $f(X_0)$ to update the global optimization value xg and $f(x_g)$; otherwise, keep the global optimization value unchanged.

(10) If $n<n_0$, then n=n+1, and return to step (5); continues step (11);

(11) If $k<k_0$, then k= k+1, update the temperature T_k by temperature update function: $T_k=F(T_k\text{-}1)$， and return to step (4); Otherwise, continue step (12);

(12) Compare global optimization value $f(X_g)$ with the threshold value u, if $f(X_g)$ is less than u, keep the global optimization value unchanged and terminate the algorithm . Otherwise, use the current optimization value X_g and $f(X_g)$ to update the global optimization value X_0 and $f(X_0)$, and return to step (3).

3. RESULTS AND DISCUSSION

The approach is applied in the Dagang-Zaozhuang oil pipeline safety monitoring system which covers a monitoring distance of 43km. The key parameters are $T_0=1$, p=0.8, s=1.10, $k_0=5$, $n_0=4$, u=0.1, which are gained through the field experiment.

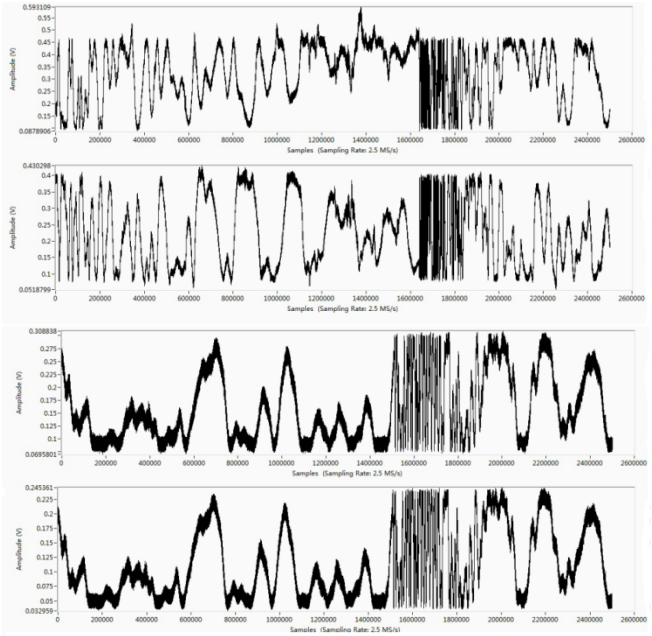

FIGURE 4: DETECTED SIGNAL WAVEFORMS. (A) POLARIZATION CONTROL IS NOT APPLIED. (B) POLARIZATION CONTROL IS APPLIED

Fig. 4 shows the contrast between the detected signal without any polarization controls and the signal detected with proposed algorithms. The signal in Fig. 4(a) has a calculated correlation coefficient ρxy=0.38, with the employment of the proposed polarization control algorithms, the correlation coefficient between the signals in Fig. 4(b) is 0.93.

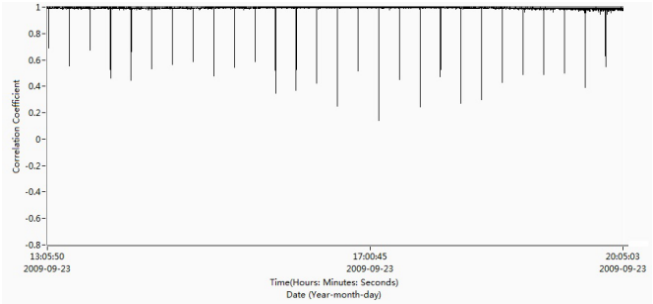

FIGURE 5: CORRELATION COEFFICIENTS WITHIN 24 HOURS. (A) POLARIZATION CONTROL IS NOT APPLIED. (B) POLARIZATION CONTROL IS APPLIED.

Fig. 5 shows the contrast of correlation coefficient within 24 hours recorded every second between before and after using the polarization control method. When correlation coefficient decreases due to external vibration or polarization state drift, the algorithm can find the new polarization operating point in a short time and regain the strong correlation between signals. To study the stability of the polarization control algorithm, the signal correlation coefficient of each second is record. Fig.6 shows the daily mean and standard deviation of the correlation coefficient. And the "SA" is under the polarization control algorithm proposed above, while the "NO SA" is without control. For comparison, Fig. 8 shows the polarization control records in one month, using the local search algorithm (LSA), genetic algorithm (GA) and simulated annealing algorithm (SA). „Control number" stands for the sequence number to manipulate computing process, while „control step" stands for the loop count for each polarization control execution.

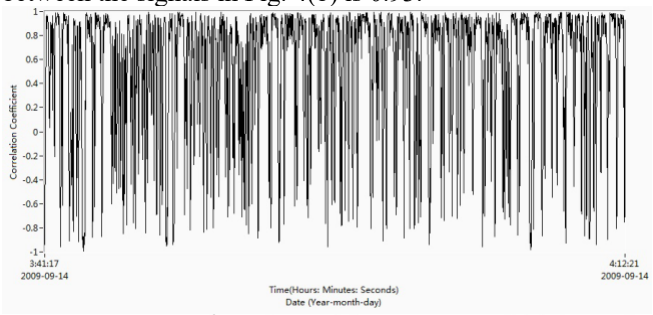

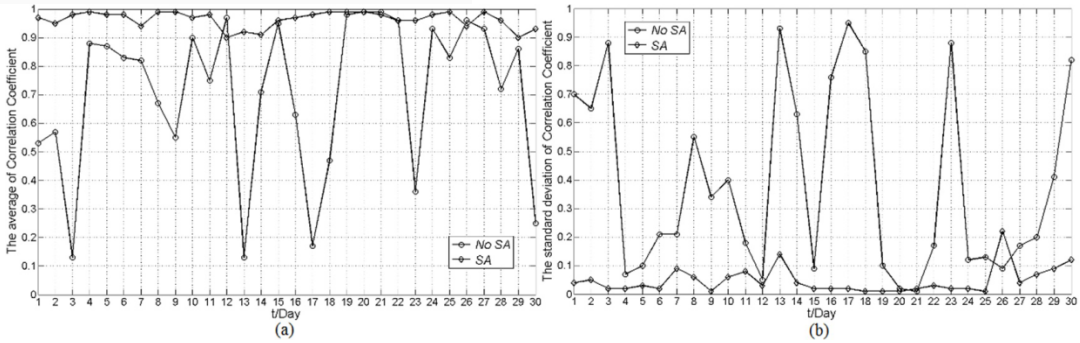

FIGURE 6: (A) THE DAILY AVERAGE OF CORRELATION COEFFICIENT BEFORE AND AFTER POLARIZATION CONTROL. (B)THE STANDARD DEVIATION OF CORRELATION COEFFICIENT BEFORE AND AFTER POLARIZATION CONTROL

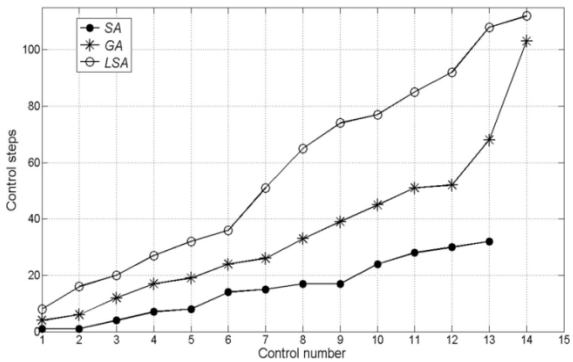

FIGURE 7: CONTROL RECORDS OF THREE ALGORITHMS

Local search algorithm can't fulfill the polarization control requirement due to its insensitivity to global convergence involving several stationary points. It fails twice a month on average, while working with low efficiency in successful trials, where the maximal control step exceeds 100 times. On the other hand, genetic algorithm needs a considerable population quantity whose diversity decreases with cross generation's growth in despite of satisfying the polarization control requirement. Thus its capacity to jump out of local optimal solution is eliminated gradually and the search speed is comparably slow. According to records, genetic algorithm generally demands three algorithm courses, and up to 103 control cycles are needed to search the polarization's operation point. In contrast, simulated annealing algorithm is more efficient and fits the control requirement substantially. Normally it finds out a novel operation point by one course, in which the cycle time is the most 32 and at least 1.Then the consistency of signals is restored as well as the system stabilized. Thus it can be concluded that simulated annealing algorithm is rather efficient compared to other methods.

Based on the investigation of the origin of positioning errors, a new polarization control method using automatic polarization controller is proposed together with stimulated annealing as its control algorithm to solve the degeneration problem of detected signals‟ correlation in the dual Mach-Zehnder fiber interferometric sensing system. The field test shows that the high correlation coefficient of the two detected signals can be obtained and kept in the proposed method, and significant improvement is achieved here compared with plain correlation operation.

REFERENCES

[1] Y. Zhou, S. J. Jin, Z. M. Zeng and H. Feng, Study on the distributed optical fiber sensing technology for pipeline safety detection and location, Journal of Optoelectronics Laser,19(2008) 922-924.

[2] A. Chtcherbakov and P. L. Swart, Polarization effects in the Sagnac-Michelson distributed disturbance location sensor, Journal of Lightwave Technology. 16(1998) 1404-1412.

[3] H. Feng, L. Zhu, S. J. Jin,Z. M. Zeng, Modeling of Pipeline Leakage Detection and Prewarning System for Locating Error Analysis Based on Jones Matrix, Journal of the Japan Petroleum Institute. 52(2009) 114-119.

[4] W. Rong and L. Dupont, A feedback algorithm for polarization control using two rotatable wave plates with variable birefringence, Optics Communications. 259(2006) 603-611.

[5] Paul R HOFFMAN, Mark G.KUZYK, Position Determination of an Acoustic Burst Along a Sagnac Interferometer, Journal of lightwave technology. 22 (2) (2004) 494-498

[6] M. Martinelli and R. A. Chipman, Endless polarization control algorithm using adjustable linear retarders with fixed axes, Journal of Lightwave Technology. 21(2003) 2089-2096.

[7] L. Dupont, W. Rong and J. Vivalda, Endless polarization control using two rotatable wave plates with variable birefringence, Optics Communications. 252(2005) 1-6.

[8] H. Feng, S. Jin, Z. Zeng, Y. Zhou and Z. Qu, Locating error analysis in pipeline leakage detection and prewarning system based on modeling using jones matrix, Acta Optica Sinica. 29(2009) 723-727.

[9] G. B. Gao, W. Wang, K. Lin and Z. C. Chen, Parameter identification based on modified annealing algorithm for articulated arm CMMs, Optics and Precision Engineering. 17(2009) 2499-2505.

[10] Shi, Yiwen, Dworak. Jennifer, A Simulated Annealing Inspired Test Optimization Method for Enhanced Detection of Highly Critical Faults and Defects, Journal of Electronic Testing. 3(2013) 1-4.